Available online at www.sciencedirect.com
ScienceDirect
Journal of Power Sources 159 (2006) 258–262
JOURNAL OF POWER SOURCES
www.elsevier.com/locate/jpowsour

Short communication

Oxysulfide glasses xLi_2O–$(1-x)(0.6Li_2S$–$0.4P_2S_5)$

R. Prasada Rao *, M. Seshasayee

Department of Physics, Indian Institute of Technology Madras, Chennai-600036, India

Available online 6 June 2006

Abstract

Amorphous solid electrolytes in the system xLi_2O–$(1-x)(0.6Li_2S$–$0.4P_2S_5)$ (with $x = 0.1$, 0.15, 0.2, 0.25, 0.3, 0.35 and 0.4) have been prepared from a mixture of Li_2O, Li_2S and P_2S_5 using a mechanical milling technique at room temperature and in inert atmosphere. The oxysulfide powder mechanically milled for 80 h with $x = 0.25$ shows an ionic conductivity (σ) of 2.5×10^{-4} S cm^{-1} at 300 K which is the highest in this series. The glass transition temperature (T_g) exhibits a minimum at $x = 0.25$. Constant volume molecular dynamics was done for all x. Structural and transport results from molecular dynamics (MD) simulation are described. Changes in structure with x and their influence on σ and T_g are discussed.

Keywords: Mechanical milling; Lithium ion conduction; Molecular dynamics

1. Introduction

Very few structural reports based on mechanically milled oxysulfide glasses exist [1–4]. ^{29}Si MAS-NMR and XPS studies for melt quenched glass system $(100-x)(0.6Li_2S$–$0.4SiS_2)$–xLi_xMO_y ($Li_xMO_y = Li_4SiO_4$, Li_3PO_4, Li_4GeO_4, Li_3BO_3, Li_3AlO_3, Li_3GaO_3 and Li_3InO_3) was reported by Minami et al. [5]. These studies reveal that in the systems with small amounts of Li_xMO_y, the silicon atoms coordinated with both bridging oxygen atoms and non-bridging sulfur atoms. The presence of large amounts of these unique silicon structural units brought about high conductivities and high thermal stability of these glasses. On the other hand, presence of non-bridging oxygen atoms and S^{2-} units created by large amounts of Li_xMO_y, lowered these excellent properties. Crystallization kinetics and structural changes during crystallization of $(100-x)(0.6Li_2S$–$0.4SiS_2)$–xLi_3PO_4 oxysulfide glasses were investigated by Hayashi et al. [6]. The composition dependence of the activation energy showed opposite variation to the difference $T_c - T_g$, where T_g and T_c are the glass transition and crystallization temperatures, respectively. This inverse correlation was explained in terms of the fragility of the glasses studied. Solid state MAS-NMR measurement revealed that silicon and phosphorus atoms coordinating with both sulfur and oxygen atoms present in oxysulfide glasses were not detected after crystallization. In mechanical milling, when Li_2O and P_2O_5 were separately used as oxygen source in Li_2S–P_2S_5 system [7], the authors found that P_2O_5 reacted more effectively compared to Li_2O in the formation of glass. In order to understand the short range order around P and Li atoms and the emerging structural changes due to the addition of Li_2O, molecular dynamics study of xLi_2O–$(1-x)(0.6Li_2S$–$0.4P_2S_5)$ with $x = 0.1$, 0.15, 0.2, 0.25, 0.3, 0.35 and 0.4 was taken up and reported here. To analyze the MD generated configuration of atoms, graph theory techniques [8,9] were used to completely elucidate the connectivities of the various units present and their ratios. Statistics of chains and rings present were also calculated using this technique.

2. Glass preparation and characterization

The starting materials, Li_2O, Li_2S and P_4S_{10} (Aldrich, 99%) were placed in an agate pot of volume 50 ml with 10 agate balls of 10 mm diameter and 2 agate balls of 8 mm diameter. The mechanical milling was conducted using a high-energy ball mill at room temperature. The rotation speed of base and bowl was fixed at 380 rpm. The ball to mixture weight ratios were in between 10 and 20. All the processes were carried out in a glove box that was filled with dry nitrogen gas. The diffractogram taken at the start of the milling process for the glass with $x = 0.2$ showed peaks due to Li_2O, Li_2S and P_4S_{10} (Fig. 1). At the end of 80 h of milling all the peaks disappeared leaving a halo pattern. Fig. 2 shows the X-ray diffraction of some of the glasses after 80 h of milling. The density of these powders were measured using Archimedes principle taking toluene

* Corresponding author.
E-mail address: prasadarao@physics.iitm.ernet.in (R.P. Rao).

0378-7753/$ – see front matter © 2006 Elsevier B.V. All rights reserved.
doi:10.1016/j.jpowsour.2006.04.031

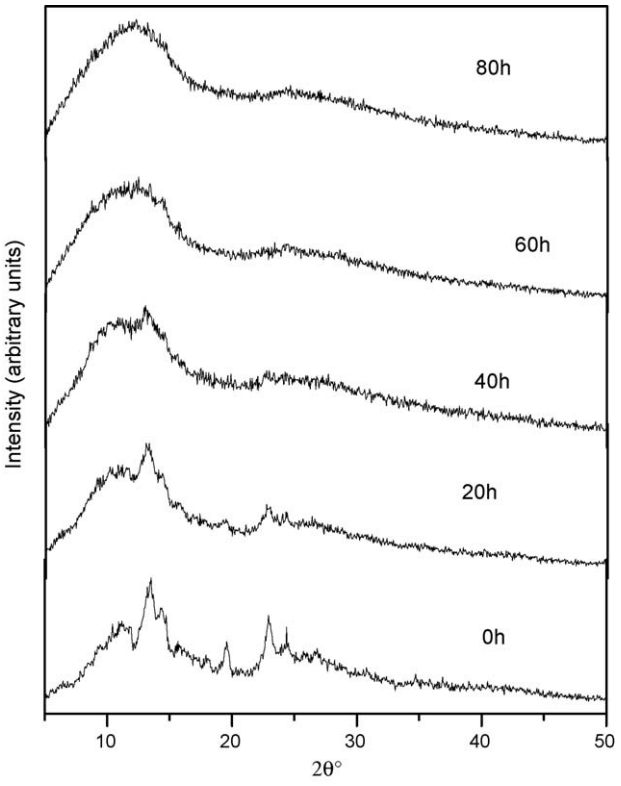

Fig. 1. XRD of $0.2Li_2O–0.8(0.6Li_2S–0.4P_2S_5)$ with different periods of milling.

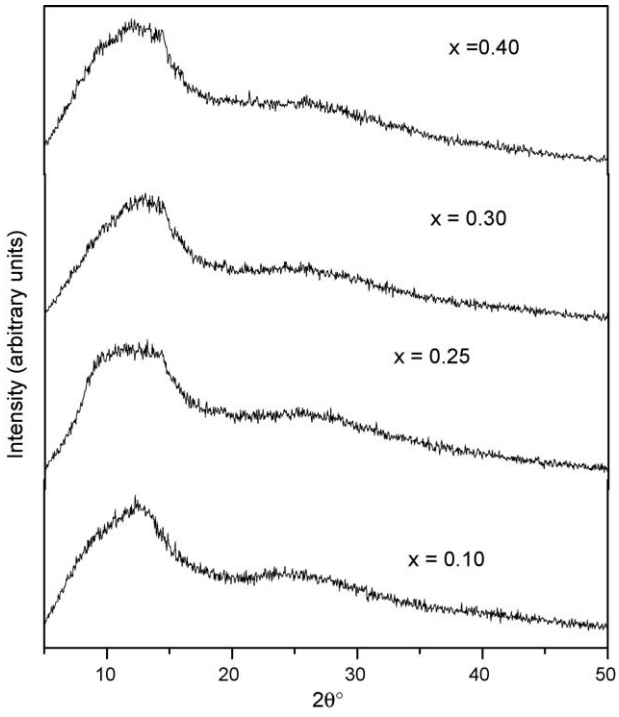

Fig. 2. XRD of $xLi_2O–(1-x)(0.6Li_2S–0.4P_2S_5)$ after 80 h of milling.

(density 0.863 g cm^{-3}) as the immersing medium (Table 1). Ionic conductivity measurement was done at room temperature by Keithley 3330 impedance analyzer in the frequency range 40–100 kHz. Pellets of the sample of size 12 mm (diameter) × 2 mm (thickness) were made using Ag powder on both sides of the sample and applying a pressure of 3 tonnes. DC conductivity was calculated from the plot of $\log f$ versus $\log \sigma$, by extrapolating the frequency independent plateau region to zero frequency. The glass transition temperature, T_g was obtained using a NETZSCH DSC 200 PC, at a heating rate of 10 °C min^{-1} under constant flow of high pure N_2 gas. Measured values of density, σ and T_g are given in Table 1 and in Figs. 3 and 4.

3. Molecular dynamics (MD) simulation

Constant volume MD was performed on cubic cells calculated with measured densities (Table 1). Starting at a temperature

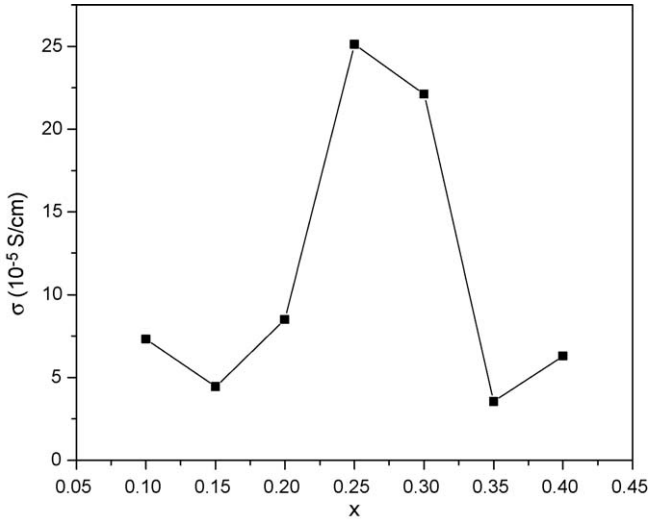

Fig. 3. Variation of measured T_g with x for $xLi_2O–(1-x)$ $(0.6Li_2S–0.4P_2S_5)$ system.

Table 1
Physical parameters for $xLi_2O–(1-x)(0.6Li_2S–0.4P_2S_5)$ system

Parameter	Density (g cm^{-3})	σ (experimental) ($\times 10^{-4}$ S cm^{-1})	T_g (experimental) (K)	σ (MD) ($\times 10^{-2}$ S cm^{-1})	T_g (K) (MD)
$x=0.10$	1.86	0.73	382.5	23.55	476
$x=0.15$	1.89	0.44	384.6	8.24	485
$x=0.20$	1.92	0.85	386	29.59	508
$x=0.25$	1.86	2.51	381	48.31	467
$x=0.30$	1.82	2.21	388	30.44	520
$x=0.35$	1.72	0.35	386.6	3.82	495
$x=0.40$	1.79	0.63	386	43.82	502

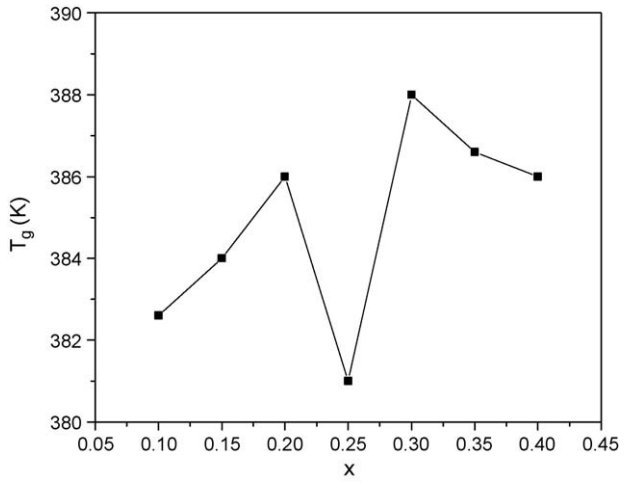

Fig. 4. Variation of measured σ with x for $0.2Li_2O–0.8(0.6Li_2S–0.4P_2S_5)$ system.

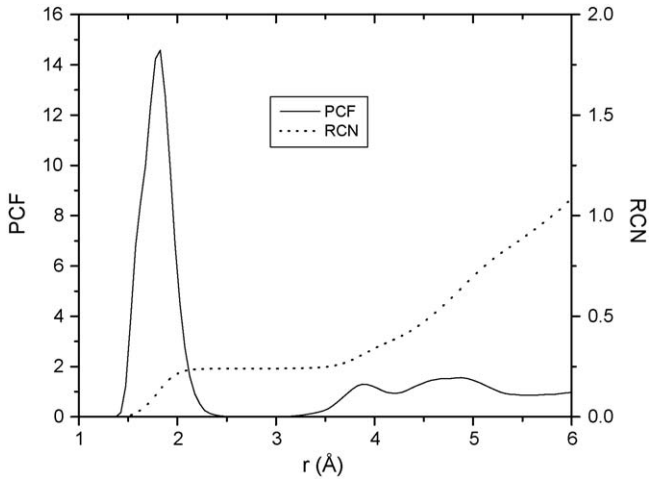

Fig. 5. PCF and RCN of P–O for $0.2Li_2O–0.8(0.6Li_2S–0.4P_2S_5)$ at 300 K.

of 3000 K, the system was cooled by scaling velocities to 2000 K, 1500 K, 1000 K, 750 K, 600 K, 350 K and finally to 300 K with time step size of 10^{-15} s. At each temperature, the system was equilibrated for 20 ps and various parameters such as pair correlation function (PCF) and running coordination number (RCN) for various atomic pairs were averaged for another 80 ps. At 600 K, 350 K and 300 K, the equilibration and averaging times were increased to 100 ps each. The interatomic potential used was of the form

$$\phi_{ij} = \frac{Z_i Z_j e^2}{r_{ij}} + A_{ij} \exp\left(\frac{-r_{ij}}{\rho_{ijo}}\right) + \frac{k_{ij}}{8(\theta_{jik} - \pi)^2} \times \left\{\left[(\theta_0 - \pi)^2 - (\theta_{jik} - \pi)^2\right]^2\right\} \exp\left[-\left(\frac{r_{ij} + r_{ik}}{\rho_{ij}}\right)\right]$$

where Z_i is the atomic number of atom i and θ_0 is the equilibrium angle subtended by r_{ij} and r_{ik}. A_{ij}, ρ_{iio}, k_{ij} and ρ_{ij} are constants of simulation. The third term in the potential is the three body vessel term introduced to account for the covalent nature of interactions. Z_i for Li, P, O and S are 0.4e, 2e, −0.8e and −0.8e, respectively. Initial values for constants of simulation and atomic number Z_i were obtained from MD studies reported for the binary systems $xLi_2S–(1-x)P_2S_5$ [10]. They were subjected to further adjustments till equilibrium was attained at all simulated temperatures with chemically acceptable bond lengths. Table 2 contains the relevant potential parameters used.

Table 2
Potential parameters used in two body Buckingham term for $xLi_2O–(1-x)(0.6Li_2S–0.4P_2S_5)$ system

Parameter	A_{ij} (eV)	ρ_{ijo} (Å)
P–P	4000.91	0.35
P–O	190.0	0.36
P–S	1000.57	0.288
S–S	4200.43	0.27
Li–S	1000.42	0.26
Li–O	200.0	0.28

To calculate the mean square displacement [MSD] for all atoms, the averaging time was increased to 100 ps at all temperatures. The diffusion constant D for Li^+ was obtained from the slope of the linear part of the mean square displacement versus time interval (τ) curve. This follows from the Einstein's equation,

$$D = \frac{1}{6}\frac{d}{d\tau}\left\langle [r(t_0) - r(t_0 + \tau)]^2 \right\rangle$$

where $\left\langle [r(t_0) - r(t_0 + \tau)]^2 \right\rangle$ is the MSD, τ the time interval and $\langle \cdots \rangle$ indicates average over time origins.

T_g, the glass transition temperature was obtained from the change in slope in the D (for Li^+) versus temperature plot. The structure of the simulated glass was analysed from connectivity matrices and graph theory techniques as reported by us earlier [11,12] and averaged over 50 different equilibrated configurations at 300 K.

4. Results and discussion

PCF and RCN for P–O are shown in Fig. 5 at 300 K. MSD versus time interval (τ) for Li, P, O and S are shown in Fig. 6 for $x = 0.4$ at 300 K. Such plots for other glasses are similar. σ and T_g obtained from MD are given in Table 1. Analysis of the equilibrium configuration from MD using the adjacency matrix yielded parameters in Table 3. In this table, r_{i-j} denotes the average distance between atoms i and j and n_{i-j} denotes the average number of j atoms around an i atom. BO represents oxygens in P–O–P. NBS represents sulfurs that do not take part in P–S–P bridging, but do take part in P–S–Li type of linkage to varying extent. P–Li–Li–P denotes linkages among various P–S–P chains mediated by Li as P–S–Li–S–Li–S–P.

The total coordination including O and S around P is close to 5. Around Li, it varies between 3.5 and 4.77. Two peaks are found in P–P PCF at 3.67 Å and 4.2 Å for all glasses. These peaks arise from P–O–P and P–S–P interactions. They are of varying heights due to changing fractions of these bridges. All distances r_{i-j} show little variation with x, with exception of $r_{P–O}$ which has large values for $x = 0.1$ and 0.15. This is also observed

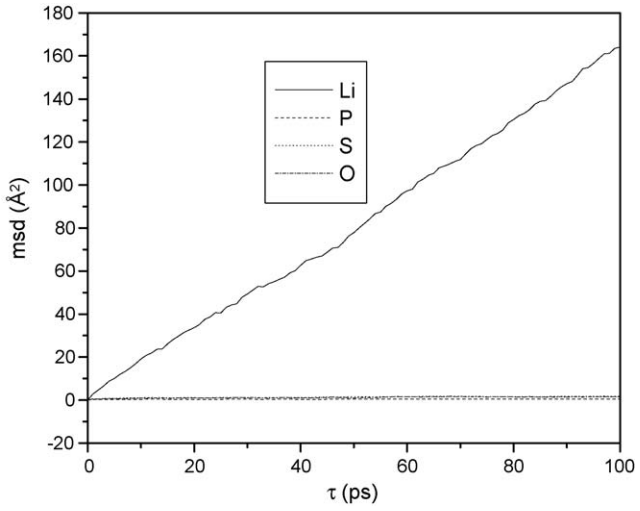

Fig. 6. MSD vs. τ for $0.4Li_2O$–$0.6(0.6Li_2S$–$0.4P_2S_5)$ at 300 K.

in a similar system xLi_2O–$(1-x)P_2S_5$ [13] which occurs for a low ratio of $n_{P–O}/n_{P–S}$, the reasons for which is not clear.

The coordination around P is made up of units such as PS_5, POS_4, PO_2S_3 and PS_3 in varying fractions for the different compositions. The reported unit POS_3 at the composition for the highest sigma found in the glass Li_2S–P_2S_5–P_2O_5 [7] also occurs in this system at $x=0.20$, which is close to the maximum conductivity region of $x=0.25$. For all compositions, nearly equal fractions of LiS_3 and LiS_4 units are found around Li with minor fraction of LiS_5. For x greater than 0.25, units such as $LiOS_2$, $LiOS_3$ and $LiOS_4$ units are found in smaller numbers. Chain structure exists, made up of P–S–P chains. The average chain length decreases from 11.4 to 8.8 at $x=0.25$ and then increases to 12.9 at $x=0.4$. The average chain length made up of P–O–P bridges is slightly above 1 and varies between 1.03 and 1.38 which shows that P–O–P chains do not exist.

T_g variations with x for measured and simulated data are given in Table 1. Their increase and decrease with x follow the same order except at the end between $x=0.35$ and 0.4. The fraction of bridging oxygens which strengthens the glass has a minimum at $x=0.25$ and understandably the T_g also has a minimum there. The rise and fall of σ with x is similar for the simulated and measured data except at $x=0.4$, where the simulated σ shows a sharp increase. Simulated σ is three orders of magnitude higher than those of the measured glasses. Higher σ is generally observed in simulated glasses due to high fictive temperatures caused by the very high cooling rate in simulation (10^9 K s^{-1}). Ball milled glasses have even lower cooling rate compared to quenched glasses which gives rise to the large difference in sigma observed here.

Inspection of Table 3 shows that many structural changes are taking place at $x=0.25$, in addition to the maximum in σ and the minimum in T_g both of which occur for $x=0.25$. Structural changes observed at $x=0.25$ and their causes are given below:

(1) $n_{P–S}$ remains high up to 0.25 and then decreases and $n_{Li–S}$ becomes a maximum. Three factors contribute to this coordination behaviour. Both Li and P share the sulfurs, P/S ratio remains at 0.307 and #(Li + P)/#S ratio becomes greater than 1 for $x>0.25$, giving rise to lower $n_{P–S}$ and $n_{Li–S}$ at higher x.
(2) Both Li–O–P and Li–S–P have maximum values. The fraction of NBOs having more than one Li around them is maximum (0.33(3)) for $x=0.25$ resulting in the maximum for Li–O–P interaction. The fraction of bridging oxygens interacting with Li is negligibly small for all x. But for sulfur, the opposite happens. The fraction of BS having more than one Li around it is maximum for $x=0.25$ which causes the maximum value in Li–S–P.
(3) The average P–S–P chain length is a minimum even though it coincides with the minimum in NBS population. Short P–S–P chains with smaller NBS population is possible if the chains possess many branches which leads to higher M_n for n less than the chain length. For $x=0.25$, the average chain length is 8.8 and its M_6 is on the higher side.

Table 3
Parameters obtained from graph theory analysis for xLi_2O–$(1-x)(0.6Li_2S$–$0.4P_2S_5)$ system

Parameter	$x=0.10$	$x=0.15$	$x=0.20$	$x=0.25$	$x=0.30$	$x=0.35$	$x=0.40$
$r_{P–O}$ (Å)	1.82	1.82	1.62	1.59	1.62	1.62	1.62
$r_{P–S}$ (Å)	2.12	2.12	2.12	2.15	2.15	2.15	2.15
$r_{Li–O}$ (Å)	2.07	2.07	2.07	2.06	2.07	2.07	2.07
$r_{Li–S}$ (Å)	2.52	2.52	2.52	2.52	2.52	2.52	2.52
$n_{P–O}$	0.214(6)	0.286(9)	0.419(7)	0.493(9)	0.68(1)	0.80(1)	0.93(1)
$n_{P–S}$	4.65(1)	4.54(2)	4.53(2)	4.66(2)	4.27(1)	4.04(2)	4.03(3)
$n_{Li–O}$	0.050(4)	0.109(9)	0.156(7)	0.30(1)	0.26(1)	0.34(1)	0.44(1)
$n_{Li–S}$	3.60(3)	3.50(3)	3.63(3)	4.47(2)	3.38(3)	3.18(3)	3.19(2)
BO	0.54(4)	0.38(2)	0.36(2)	0.24(1)	0.31(2)	0.25(1)	0.17(1)
NBS	0.449(5)	0.474(9)	0.489(5)	0.451(6)	0.569(7)	0.614(1)	0.609(1)
S^{2-}	0.031	0.046	0.046	0.052	0.048	0.062	0.071
#(Li–O–P)/#O	1.6(1)	1.9(1)	2.2(1)	3.6(1)	2.7(1)	3.0(1)	3.4(1)
#(Li–S–P)/#S	10.6(1)	10.9(1)	12.3(1)	18.7(1)	13.0(1)	12.7(2)	14.4(1)
Average (P–S–P) chain length	11.4(3)	10.3(4)	10.8(5)	8.8(3)	12.8(7)	12(1)	12.9(2)
Average (P–O–P) chain length	1.17(3)	1.037(3)	1.23(2)	1.14(4)	1.38(1)	1.359(9)	1.49(6)
S/O	23.4	14.73	10.4	7.86	6.06	4.82	3.9

$r_{i–j}$ values are the peak values obtained from MD.

(4) T_g registers a minimum where the BO population shows a dip though it does not have a minimum there. To explain this behaviour of T_g at all x, it is necessary to take the oxygen content (OC) of the glass into account as well. If G denotes the product of BO and OC, then the behaviour of G with x is similar to that of T_g.

(5) σ is maximum. For the compositions we have studied here, the BO population is high for x less than 0.25 and NBS population is high for x greater than 0.25. The S^{2-} fraction increases mildly with x. The first two parameters have low values for $x = 0.25$ and yet σ attains maximum value there. However, for this composition, the average number of Li^+ found near BO and the corresponding number for BS have maximum values of 0.11 and 0.82 among all other compositions, which creates a very conducive environment for higher Li mobility. At $x = 0.4$, the NBS population is on the higher side, though the other factors are not so favourable. Hence its high σ can only be attributed to the large NBS population found there. It is pertinent to add here that the measured σ does not show such a high value for $x = 0.4$.

It is seen that for the ratio of sulfur to oxygen content (S/O) between 6 and 7.8, experimental σ has the highest range of values between 2.21 and 2.51×10^{-4} S cm^{-1}. High values in this range are also obtained for σ from MD if we neglect the high σ at $x = 0.4$ which is not seen in experimental σ. For oxysulfide glass systems $(100 - x)(0.6Li_2S–0.4SiS_2)–xLi_xMO_y$ ($Li_xMO_y = Li_4SiO_4$, Li_3PO_4 and Li_4GeO_4), σ is highest for S/O equal to 6.65 and for $Li_xMO_y = Li_3BO_3$, Li_3AlO_3, Li_3GaO_3 and Li_3InO_3, the highest σ is obtained for S/O equal to 8.8 [5]. These values of S/O fall in the range for high σ obtained for our system. It is surprising that for such different systems with varying coordinations and basic units in the glass matrix, σ seems to depend crucially on S/O ratio. In $Li_2S–P_2S_5–P_2O_5$ glass prepared by mechanlcal milling, the highest σ is obtained in $80Li_2S–19P_2S_5–1P_2O_5$,where the S/O ratio equals 35. Higher P_2O_5 content reduces σ in this system [7]. This result shows that the source of oxygen matters in addition to its fractional content in the glass.

5. Conclusions

Both P and Li coordinate to O as well as S atoms in various proportions in this system. The BO, NBS and S^{2-} populations control the conductivity. Many significant changes occur at $x = 0.25$ where the highest conductivity and the lowest T_g are observed.

References

[1] S. Kondo, K. Takada, Y. Yamamura, Solid State Ionics 53–56 (1992) 1183–1186.
[2] K. Takada, N. Aotani, K. Iwamoto, S. Kondo, Solid State Ionics 86–88 (1996) 877–882.
[3] H. Morimoto, H. Yamashita, M. Tatsumisago, T. Minami, J. Am. Ceram. Soc. 82 (5) (1999) 1352–1354.
[4] M. Tatsumisago, H. Yamashita, A. Hayashi, H. Morimoto, T. Minami, J. Non-Cryst. Solids 274 (2000) 30–38.
[5] T. Minami, A. Hayashi, M. Tatsumisago, Solid State Ionics 136–137 (2000) 1015–1023.
[6] A. Hayashi, M. Tatsumisago, T. Minami, J. Non-Cryst. Solids 276 (2000) 27–34.
[7] F. Mizuno, T. Ohtomo, A. Hayashi, K. Tadanaga, T. Minami, M. Tatsumisago, J. Cerm. Soc. Jpn. 112 (5) (2004) S709.
[8] F. Harary, Graph Theory, Narosa Publications, 1988.
[9] N. Trinajstic, Chemical Graph Theory, CRC Press, Boca Raton, FL, 1992.
[10] R.K. Sistla, M. Seshasayee, J. Non-Cryst. Solids 349 (2004) 22–29.
[11] D.M. Cvetkovic, I. Gutman, Croat. Chem. Acta 49 (1) (1977) 115–121.
[12] R. Prasada Rao, M. Seshasayee, Solid State Commun. 131 (8) (2004) 537–542.
[13] R. Prasada Rao, M. Seshasayee, submitted for publication.